Simulation of a Typhoon Event with Assimilated GPS Refractivity from FORMOSAT-3/COSMIC Using a Nonlocal Operator of WRF 3DVAR

Shu-Ya Chen[1], Ching-Yuang Huang[1], Ying-Hwa Kuo[2,3], Yong-Run Guo[3] and Sergey Sokolovskiy[2]

[1]Department of Atmospheric Sciences, National Central University, Jhongli, Taiwan
[2]University Corporation for Atmospheric Research, Boulder, Colorado, USA
[3]National Center for Atmospheric Research, Boulder, Colorado, USA

Abstract

A nonlocal operator has been used to assimilate GPS radio occultation (RO) refractivity with WRF 3DVAR. For comparisons, the ray path can be localized by confining the ray near the RO point as a localized nonlocal operator, which is equivalent to the conventional local operator. All of the nonlocal, localized-nonlocal and local operators were applied to assimilate GPS RO refractivity soundings available from FORMOSAT-3/COSMIC for WRF simulations of Typhoons Kaemi in July 2006 that impinged Taiwan with torrential rainfall. The initial increments produced by both nonlocal and localized-nonlocal operators are quite similar in distribution. However, the increments for the nonlocal operator are more stretched along the ray's direction, as a result of the integration effect. During 72-h integration, the assimilation by the nonlocal operator shows the best simulated track as compared to the best track in the first day. The patterns of simulated daily accumulated rainfall are similar for runs with and without assimilation, however the run without assimilation produces larger and wider rainfalls in later simulation time than the assimilation runs, as compared to the observations. Both assimilation runs also produce too much rainfall in the third day, but such over-prediction is reduced in the assimilation run with GPS RO data.

1. Introduction

The atmospheric refractivity (N) can be related to pressure, temperature and water vapor pressure of the atmosphere. Assimilation with the Abel-retrieved refractivity data has assumed local measurement at the perigee point where the GPS ray is closest to the earth (e.g., Huang et al. 2005; Sokolovskiy et al. 2005). This treatment also indicates that the observed refractivity is used as a local model value, as assimilated by a typical refractivity operator. However, the Abel-retrieved refractivity accounts for an integrated amount of refractivity along the path of the ray in a spherically-symmetric atmosphere. In order to take the effect of the integration into account, Sokolovskiy et al. (2005) suggested use of excess phase as the observable for assimilation, which is defined as the integrated amount of refractivity along the ray. For simplicity and efficiency, the ray has been assumed to be a straight line in the integration. Such a forward scheme is the so-called nonlocal operator as compared to the local operator using the point refractivity. The developed nonlocal operator has been implanted into the WRF 3DVAR (version 2.1).

2. The experiment designs, simulated results and discussion

The Weather Research & Forecasting (WRF) Model (version 2.1.2) was applied to simulate Typhoon Kaemi (2006). We estimate the observation errors from FORMOSAT-3/COSMIC data during 15th July to 15th August 2006 by Hollingsworth-Lönnberg method. As seen, the distributions of the observation errors for COSMIC data (Fig. 4) are similar to those from CHAMP observations during 15th August to 15th September 2003, and the latter observation error statistics are used in this study. The new assimilation operator developed for WRF 3DVAR takes into account the integration of the refractivity along the ray path, defined as excess phase $S = \int N\, dl$ where l is the ray path. Herein, some properties of the nonlocal operator should be mentioned: (1) the assimilation is performed at model mean heights for saving of computation time; (2) both observation and model refractivities are integrated by identical interpolation schemes with two constraints that confine the ray within the model domain and cannot allow penetration into a mountain; (3) the observed refractivity is assumed to be spherically symmetric about the RO point and the coordinates of the perigee point for each

ray may vary with geodetic height; and (4) the ray is presumed to be a straight line for simplicity and the integration is terminated when the ray has advanced beyond the model top which is set to 50 hPa (about 20 km).

The first guess for WRF 3DVAR was taken from the NCEP AVN analysis which also provided the boundary condition for the outermost domain. The WRF model with three nested domains (45 km, 15 km and 5 km resolutions) was initialized at 0000 UTC 23 July, within 6 h of which seven GPS RO events took place. We conducted the simulations with no assimilation (denoted by NONE) and with assimilated refractivity by both nonlocal operator and localized-nonlocal operator (denoted by EPH and LLZ, respectively) for comparisons. The only difference between the localized-nonlocal operator and the nonlocal operator is that the excess phases are bounded within one grid mesh. We also assimilated GPS RO data in the observation heights by local operator, denoted by experiment LOC. The ingestions of the seven GPS RO refractivity soundings produce initial sizable increments (the differences between the initial fields with and without the GPS assimilation) as shown in Fig. 1 for the level of 433 mb. In general, the temperature increments, moisture increments and refractivity increments for EPH, LLZ and LOC have similar geometric distributions at this level. Also, the increments for all operators appear to have same signs for most of the observation regions. We note that the shape of the moisture and refractivity increment contours for EPH is more elliptic compared to that for LLZ and LOC. The long axis of the elliptic is primarily along the ray propagation (not shown). The distributions of increments for the nonlocal operator are slightly stretched along the ray's direction, reflecting the effect of the integration.

Figure 2 shows the best track and the simulated 72-h tracks of the typhoon center (the position of minimum perturbation pressure) for the above four experiments. Without relocation of the initial typhoon center, the initial model position departs slightly from the observed. For this case, EPH shows the smallest 24-h mean track error (about 79 km) in the first day, however they are larger than 100 km for the other experiments (figures not shown). According to the distributions of increments in vertical profile (not shown), we have observed more moisture modifications at lower levels from assimilation of GPS RO soundings. It is interesting to see whether the rainfall prediction will also be impacted by the data assimilation. Figure 3 shows the 24-h accumulated rainfalls for the observations, and NONE, REF and EPH, in the second and third day simulations. When Kaemi approaches closer to Taiwan, most of the rainfalls are produced over eastern Taiwan as observed. Observations also show a pronounced rainfall maximum over southern CMR between 22.5°N and 23°N, which is not well predicted by all the four experiments. For the third day, NONE exhibits over-prediction on rainfall over Taiwan, while over-precipitation is largely reduced for the three GPS assimilation runs. The threat scores (TS) of the accumulated rainfalls are shown in Fig. 5. For this typhoon event, the TS for large rainfall amounts could be higher than 0.5 even after the third day. It was evident that EPH shows the highest TS for larger rainfalls for thresholds of 20 and 50 mm on the third day. Although TS for EPH becomes lower than NONE for small rainfall amounts, it is still better than LLZ and LOC. In general, both EPH and LLZ exhibit about the same performance early in the simulation; however, it becomes improved at later times for the former.

3. References

Huang, C.-Y., Y.-H Kuo, S.-H. Chen, and F. Vandenberghe, 2005: Improvements in Typhoon Forecasts with Assimilated GPS Occultation Refractivity. *Wea. Forecasting*, **20**, 931–953.

Sokolovskiy, S., Y.-H. Kuo, and W. Wang, 2005: Assessing the Accuracy of a Linearized Observation Operator for Assimilation of Radio Occultation Data: Case Simulations with a High-Resolution Weather Model. *Mon. Wea. Rev.*, **133**, 2200-2212.

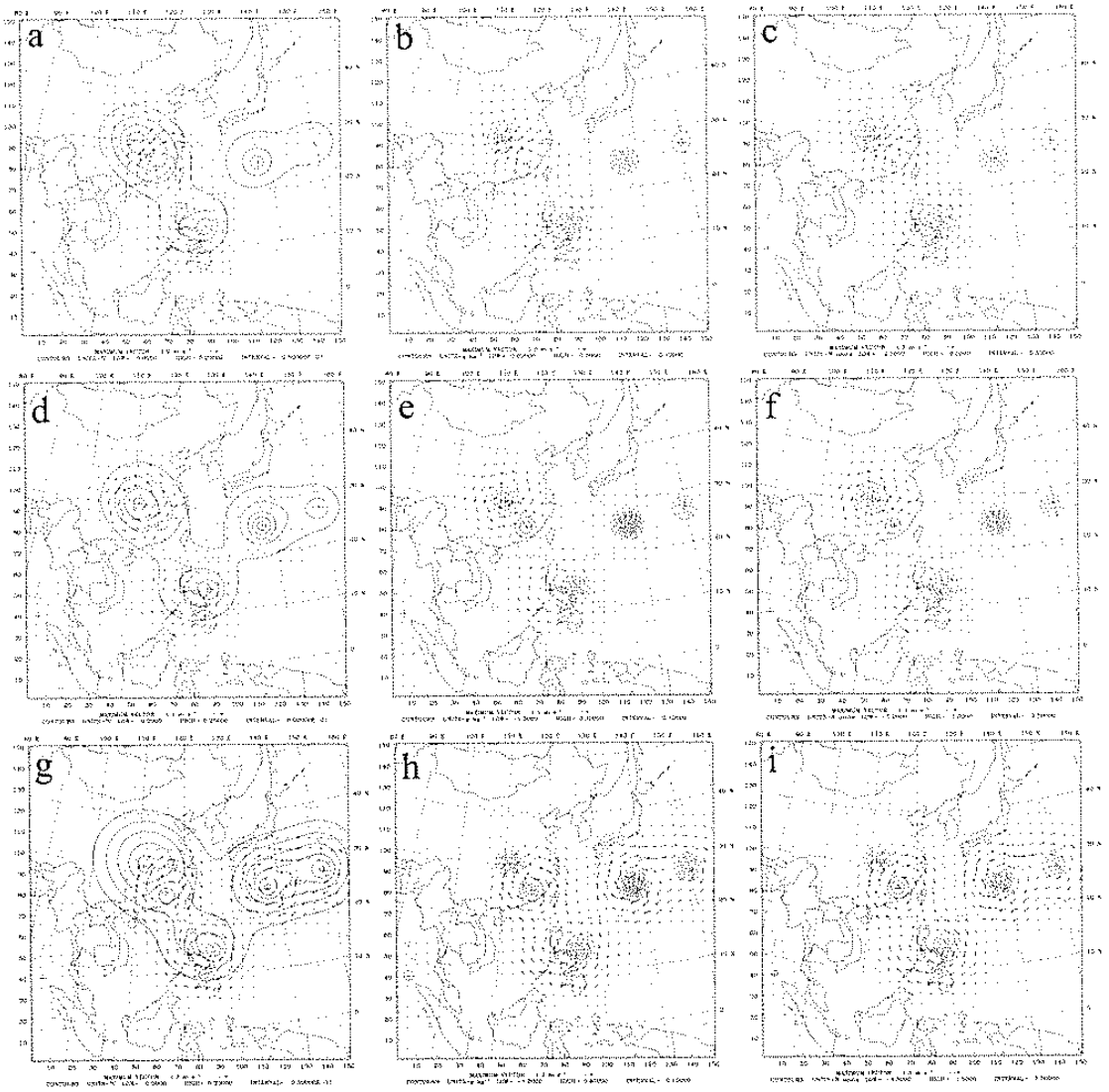

FIG. 1. Initial increments for (a) temperature (at an interval of 0.05 °C), (b) water vapor mixing ratio (at an interval of 0.1 g kg^{-1}), and (c) refractivity (at an interval of 0.5 N-units) at 433 mb produced by the nonlocal operator with the increments for horizontal wind at the same level overlapped, and (d), (e) and (f) as in (a), (b) and (c), respectively, but for the localized-nonlocal operator, and (g), (h) and (i) for local operator. The plus signs indicate the occultation positions.

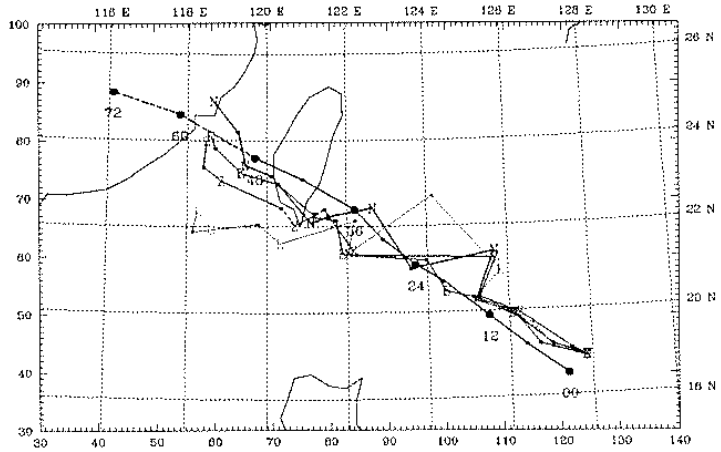

FIG. 2. The best track from CWB (marked by solid circle with 6-h interval), and the simulated tracks for the experiments NONE (denoted by "N"), LOC (denoted by "L"), LLZ (denoted by "Z") and EPH (denoted by "E").

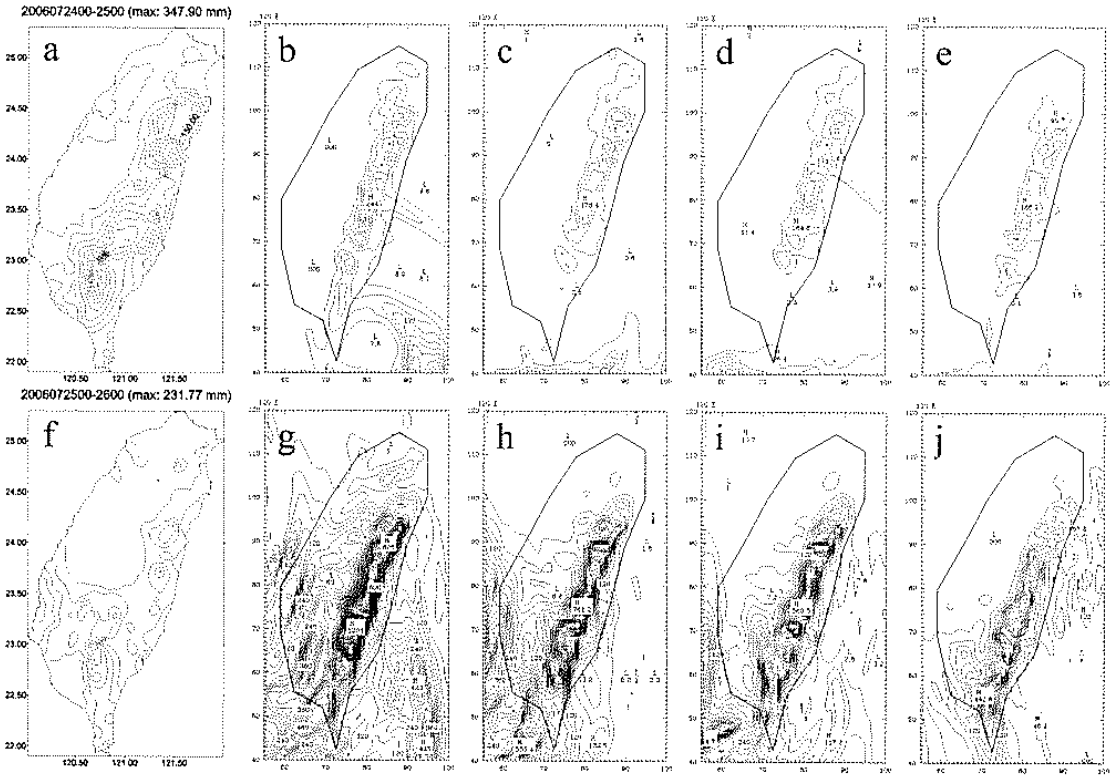

FIG. 3. The 24-h accumulated precipitation on 24 to 25 July (the second day of simulations) for (a) the observation, and the experiments (b) NONE, (c) EPH, (d) LLZ and (e) LOC. Panels (f) to (j) are the same as panels (a) to (e), respectively, but for the third day of simulations. The contour interval is 30 mm.

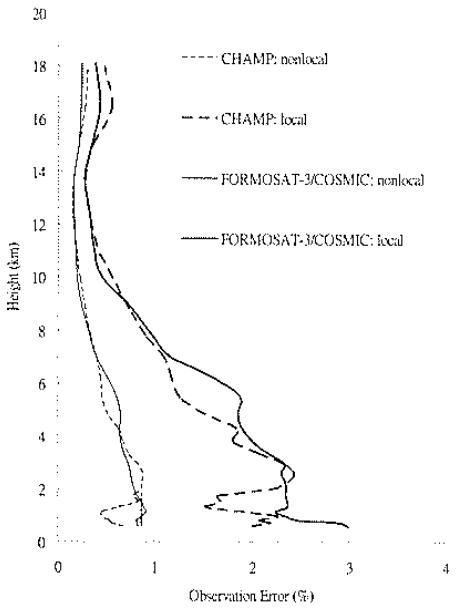

FIG. 4. The statistical observation errors by using local (right) and nonlocal (left) operators for CHAMP data are shown in dash lines and FORMOSAT-3/COSMIC data in solid lines. The dot line indicates the modified observation error for nonlocal operator below 2 km.

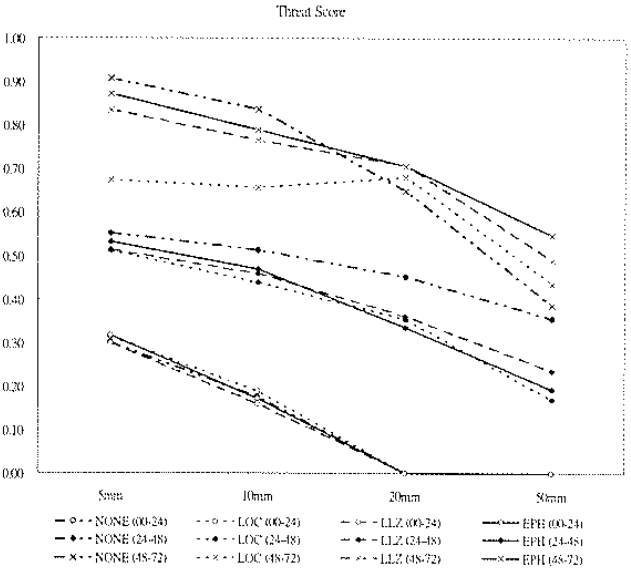

FIG. 5. The threat score of the accumulated rainfalls between 0-24 (denoted by hollow circles), 24-48 (solid diamonds) and 48-72 (cross) h varied with different thresholds for experiments NONE (dotted-dashed lines), LOC (dotted lines), LLZ (dashed lines) and EPH (solid lines).